IEEE Access
Multidisciplinary | Rapid Review | Open Access Journal

Received May 6, 2019, accepted May 23, 2019, date of publication June 3, 2019, date of current version June 13, 2019.

Digital Object Identifier 10.1109/ACCESS.2019.2920365

Discrimination of Active False Targets Based on Hermitian Distance for Distributed Multiple-Radar Architectures

QIANG LI[1], LINRANG ZHANG[1], YU ZHOU[1], SHANSHAN ZHAO[2], NAN LIU[1], AND JUAN ZHANG[1]

[1]National Laboratory of Radar Signal Processing, Xidian University, Xi'an 710071, China
[2]College of Electronic and Optical Engineering, Nanjing University of Posts and Telecommunications, Nanjing 210023, China

Corresponding author: Linrang Zhang (lrzhang@xidian.edu.cn)

This work was supported in part by the National Natural Science Foundation of China under Grant 61671361, Grant 61601343, Grant 61731023, Grant 61871305, Grant 61801233, and Grant 61801445, in part by the Natural Science Foundation of Jiangsu Province under Grant BK20170911, and in part by the Natural Science Foundation of the Jiangsu Higher Education Institutions of China under Grant 17KJB510045.

ABSTRACT In a distributed multiple-radar architecture, the spatial scattering properties of targets can be utilized to counter active deception jamming effectively. When the cooperative detection is performed, the available method to discriminate active false targets needs to know the precise jammer location, and its performance will suffer significant deterioration with little location error. Aiming at the problem, we propose a novel method to discriminate false targets based on Hermitian distance. The difference in spatial scattering property leads to the difference in the Hermitian distances of different target combinations. The Hermitian distance between two false targets is much greater than that between two physical targets or that between a physical target and a false target, especially in high jamming-to-noise ratio. Based on the difference, hypothesis testing is performed to discriminate false targets. The proposed method does not require any prior information about the jamming environment and can discriminate the targets effectively in one pulse repetition interval. Moreover, the proposed method can restrict the upper bound of the misjudgment probability for physical targets. The theoretical analysis and simulation verify the feasibility and validity of the proposed discrimination method.

INDEX TERMS Active false targets discrimination, deception electronic counter-countermeasure, distributed multiple-radar architecture, Hermitian distance.

I. INTRODUCTION

Due to its high energy efficiency and satisfactory jamming performance, active deception jamming has been playing an increasingly important role in the radar electronic countermeasure (ECM) with the development of digital radio frequency memory (DRFM) technology [1], [2]. By replicating and retransmitting the intercepted radar signal or similar radar signal after appropriate delay and modulation, active deception jamming is to produce false targets, mixing the false and physical targets to cheat or confuse hostile radars. As the contradictory of ECM, the electronic counter-countermeasure (ECCM) provides an important guarantee for the survival and operation of radars in complicated electromagnetic jamming environment [3].

Although mono-static radar has been equipped with various ECCM techniques [4]–[10], the distributed multiple-radar system, benefitting from the construction features and information fusion technology, has incomparable advantages over mono-static radar in countering deception jamming [11]. The ECCM issue in distributed multiple-radar architecture has attracted the attentions of numerous researchers, and many methods have been proposed to suppress or discriminate the active false targets which can be classified into two categories. The first category is based on the fusion processing of targets' measurements obtained in local radars. Physical targets possess spatial geometric correlation in a unified coordinate system, whereas it is usually the opposite

The associate editor coordinating the review of this manuscript and approving it for publication was Guolong Cui.

for false targets. Based on the difference, measurement fusion is performed in [12] and [13] to identify false targets. Beyond the difference above, a physical target's Doppler frequencies are not equal generally in different receivers with different view angles, which is Doppler diversity property of physical targets. By contrast, taking no account of the effect of the jammer's velocity, the Doppler of false target are near-identical in different receivers. Doppler diversity of physical targets is exploited to counter velocity-deception jamming in [14]. But a physical target will be judged as a false target if its Doppler frequency measured by multiple receivers is equal. According to Doppler diversity and spatial geometric correlation property of physical targets, the false targets are discriminated successively in Doppler domain and range domain [15]. These methods do not give full play to the potential of distributed multiple-radar architecture to counter active deception jamming, making no use of other useful information about targets except measurements.

The other category mainly makes use of the difference in signal level between physical and false targets. In a distributed multiple-radar architecture, physical targets' echoes are decorrelated among multiple receivers due to the spatial variations of radar cross section (RCS) [16], [17], while the false targets' echoes received by multiple receivers are highly correlated for one same signal resource, which is called as the difference of spatial scattering property between physical and false targets. With the same physical target's echoes noncoherent and partially coherent among multiple receivers, two methods are present respectively in [18] and [19] to discriminate false targets from fast fluctuating targets. But these methods require echo data during several consecutive pulse repetition intervals (PRIs). Therefore, it is essential to perform the discrimination of false targets within one PRI. Based on the difference in amplitude ratios of physical and false targets caused by spatial scattering property, a clustering analysis method is proposed to discriminate false targets within one PRI [20]. However, the clustering analysis method requires a higher jamming-to-noise ratio (JNR) to obtain an expected discrimination performance. A jamming cancellation method is proposed to suppress the active false targets based on the coherent property of jamming signal in [21]. Besides some processing details are not dealt with, the secondary target will be discriminated as a physical target when it happens to have similar time delays in other receivers according to the reference receiver.

Since all methods mentioned above make use of the information (including the measurements, complex amplitude, and other information about targets) obtained by independent detection of local radars, the detection performance in local radars has significant effect on their practical application. Considering a distributed multiple-radar architecture with cooperative detection performed, Shanshan Zhao creatively discusses a new manifestation of the difference of targets' spatial scattering property in [22], which can be concluded as that all signal vectors of false targets generated by one same jammer always exist in a rank one subspace, whereas physical targets' signal vectors distribute randomly in the whole space. Making use of the difference, a two-block detection/discrimination ECCM scheme is proposed based on the generalised likelihood ratio test. Its discrimination performance relies on the projection matrix, called as the jamming feature matrix, while the later depends on the precise estimation of jammer's position. When there are location errors, its discrimination performance will suffer significant deterioration, which limits its practical application. Under the same architecture, although the variance of channel energy of a physical target is much different from the one of a false target, the corresponding methods based on the difference of the variances require more research considering that it is very difficult to find the distributions of the variances.

In this paper, also in a distributed multiple-radar architecture with cooperative detection performed, aiming at the problem that the available method is dependent on the accurate location for the jammer, the Hermitian distance, defined as the cosine squared of the Hermitian angle between two complex vectors, is taken as the correlation metric to measure the mutual correlation property between two targets. It is found that the Hermitian distance between two false targets is much greater than that between two physical targets or that between a physical target with a false target, especially in high JNR. The Hermitian distance between two false targets increases with JNR and is independent of the modulation of false targets. Whereas, The Hermitian distance between two physical targets and the one between a physical target and a false target obey an identical Beta distribution which has nothing to do with signal or jamming power but the channel number. Based on the difference, a new discrimination method is proposed in this paper. The proposed method does not require any prior information about the jamming environment and can discriminate the targets effectively in one PRI. Moreover, the proposed method can restrict the upper bound of the misjudgement probability for physical targets.

The rest of the paper is organised as follows. Section II introduces the signal model for multi-radar architectures with deception jamming. The correlation property of different target combinations is analysed in details in Section III. In Section IV, the discrimination method is proposed based on the correlation difference of targets. Section V presents the simulation results and Section VI concludes this paper.

II. SIGNAL MODEL

In this paper, a multiple-radar architecture considered consists of M transmitters and N receivers distributed widely over a given area. The transmitted signals are assumed approximately orthogonal and maintain approximate orthogonality for any random time delay τ [23]

$$\int s_{m_1}(t)s^*_{m_2}(t-\tau)dt \approx \begin{cases} 1, & m_1 = m_2 \text{ and } \tau = 0; \\ 0, & \text{else} \end{cases} \quad (1)$$

where $s_{m_1}(t)$ and $s_{m_2}(t)$ are the transmitted signals of the m_1th transmitter and the m_2th transmitter, respectively.

$m_1 = 1, 2, \ldots, M$ and $m_2 = 1, 2, \ldots, M$. The superscript $*$ denotes the conjugate operator. The total number of physical targets existing in the monitoring area of the multiple-radar system is K. To protect these targets, a repeater jammer implements deception jamming by delaying, modulating and retransmitting the intercepted radar signals. After the process of the jammer, false targets are generated, whose total number is Q.

The time and phase synchronisation among multiple stations is assumed accomplished [24]–[26]. The signal received by the nth receiver, denoted by $r_n(t)$, can be presented as

$$r_n(t) = e_n(t) + j_n(t) + n_n(t) \tag{2}$$

where $0 \le t \le PRT$, PRT is the length of a pulse repetition interval (PRI). $e_n(t)$, $j_n(t)$ and $n_n(t)$ are the echo signal reflected by physical targets, deception jamming signal and the internal noise respectively.The ideal physical targets echo $e_n(t)$ can be modelled as

$$e_n(t) = \sum_{k=1}^{K}\sum_{m=1}^{M} \alpha_{mn,k} s_m\left(t - \tau_{mn,k}\right) \exp\left(-j2\pi f_0 \tau_{mn,k}\right) \tag{3}$$

where $\tau_{mn,k} = R_{mTn,k}/c$ is the time delay of the kth physical target PT_k. The term c is the speed of light and λ is the wavelength. $R_{mTn,k}$ is the range along the path from mth transmitter to nth receiver via the physical target PT_k, which is the sum of $R_{mT,k}$, the range from mth transmitter to PT_k, and $R_{Tn,k}$, the range from PT_k to nth receiver, namely $R_{mTn,k} = R_{mT,k} + R_{Tn,k}$. $\alpha_{mn,k} = \lambda\sigma_{mn,k}\sqrt{P_{Tm}G_{Tm}G_{Rn}}/(4\pi\sqrt{4\pi R_{mT,k}R_{Tn,k}})$ accounts for the complex amplitude of the physical target PT_k. P_{Tm} and G_{Tm} are the transmitted power and the antenna gain of the mth transmitter, respectively. G_{Rn} is the antenna gain of the nth receiver. $\sigma_{mn,k}$ is the radar cross section (RCS) of PT_k.

The deception jamming signal $j_n(t)$ can be expressed as

$$j_n(t) = \sum_{q=1}^{Q}\sum_{m=1}^{M} \beta_{mn,q} s_m\left(t - \tau'_{mn,q}\right) \exp\left(-j2\pi f_0 \tau'_{mn,q}\right) \tag{4}$$

where the term $\beta_{mn,q} = \gamma_q\lambda\sqrt{P_J G_{Rn}}/(4\pi R_{Jn,q})$ is the complex amplitude of false target FT_q. $\tau'_{mn,q} = R_{mJn,q}/c + \triangle\tau_q$ is the actual time delay of the qth false target FT_q. $\triangle\tau_q$ and γ_q are the jammer's time delay modulation and complex random amplitude modulation with unknown distribution for the intercepted radar signals to produce the false target FT_q. Similar to the definition of $R_{mTn,k}$, $R_{mT,k}$ and $R_{Tn,k}$, $R_{mJn,q}$, $R_{mJ,q}$ and $R_{Jn,q}$ are the range along the path from mth transmitter to nth receiver via the jammer, the range from mth transmitter to the jammer, and the range from the jammer to nth receiver, respectively, when the jammer is implementing deception jamming of false target FT_q. Therefore, $R_{mJn,q} = R_{mJ,q} + R_{Jn,q}$.

The received signal in every receiver is firstly down converted and decomposed by matched-filters, yielding totally MN isolated transmitter-receiver channel signals. Then, according to the same spatial region, a sample vector $\mathbf{x}$ with a dimension of $MN\times 1$ is obtained by extracting the corresponding samples in each channel. As the analyses in [22], when the range bin is referred to the false target FT_q, the sample vector can be written as $\mathbf{x}_{|FT,q} = \boldsymbol{\xi}_{FT,q} + \mathbf{n}$, where $\boldsymbol{\xi}_{FT,q}$ is the false target signal vector of FT_q

$$\boldsymbol{\xi}_{FT,q} = \begin{bmatrix} \beta_{11,q}\exp(-j2\pi f_0(R_{1J1,q}/c + \triangle\tau_q)) \\ \beta_{12,q}\exp(-j2\pi f_0(R_{1T2,q}/c + \triangle\tau_q)) \\ \cdots \\ \beta_{mn,q}\exp(-j2\pi f_0(R_{mJn,q}/c + \triangle\tau_q)) \\ \cdots \\ \beta_{MN,q}\exp(-j2\pi f_0(R_{MJN,q}/c + \triangle\tau_q)) \end{bmatrix} \tag{5}$$

$\mathbf{n}$ is the noise vector, whose elements are assumed to be independent identically distributed (i.i.d.) complex Gaussian distribution, namely, $\mathbf{n}\sim\mathbb{CN}(\mathbf{0}_{MN\times 1}, \sigma_n^2\mathbf{I}_{MN})$. $\mathbf{0}_{MN\times 1}$ is an $MN\times 1$ all-zero vector. $\mathbf{I}_{MN}$ is an $MN\times MN$ identity matrix.

It is a fact that the time interval the jammer generating false targets within one PRI is so short that the movement of the jammer in the time can be neglected. And the jamming signals, from the same source, are fully correlated among receivers. Considering these factors, Plugging $\beta_{mn,q}$ into (5) and extracting the common terms, $\boldsymbol{\xi}_{FT,q}$ can be written approximately as

$$\boldsymbol{\xi}_{FT,q} = \Gamma_q \cdot \boldsymbol{\xi}_J \tag{6}$$

where $\Gamma_q = \frac{\gamma_q\lambda\sqrt{P_J}}{4\pi}\exp(-j2\pi f_0\triangle\tau_q)$ is the common term of the false target FT_q in multi-channel, which is called as characterization factor characterizing the false target FT_q. $\boldsymbol{\xi}_J$ is named as jamming steering vector,

$$\boldsymbol{\xi}_J = \begin{bmatrix} \sqrt{G_{R1}}/R_{J1}\exp(-j2\pi R_{1J1}/\lambda) \\ \sqrt{G_{R2}}/R_{J2}\exp(-j2\pi R_{1J2}/\lambda) \\ \cdots \\ \sqrt{G_{Rn}}/R_{Jn}\exp(-j2\pi R_{mJn}/\lambda) \\ \cdots \\ \sqrt{G_{RN}}/R_{JN}\exp(-j2\pi R_{MJN}/\lambda) \end{bmatrix} \tag{7}$$

According to (7), $\boldsymbol{\xi}_J$ depends only on the location of the jammer and the antenna gains of the receivers but not on the modulation of false targets, which is the reason why $\boldsymbol{\xi}_J$ is called as jamming steering vector. Based on (6), there is a correlation between the false targets generated by a same jammer, which will be dealt with in details in next section.

When the range bin is referred to the physical target PT_k, the sample vector can be written as $\mathbf{x}_{|PT,k} = \boldsymbol{\xi}_{PT,k} + \mathbf{n}$, where $\boldsymbol{\xi}_{PT,k}$ is the physical target signal vector of PT_k

$$\boldsymbol{\xi}_{PT,k} = \begin{bmatrix} \alpha_{11,k}\exp(-j2\pi R_{1T1,k}/\lambda) \\ \alpha_{12,k}\exp(-j2\pi R_{1T2,k}/\lambda) \\ \cdots \\ \alpha_{mn,k}\exp(-j2\pi R_{mTn,k}/\lambda) \\ \cdots \\ \alpha_{MN,k}\exp(-j2\pi R_{MTN,k}/\lambda) \end{bmatrix} \tag{8}$$

which can be rewritten as $\boldsymbol{\xi}_{PT,k} = \boldsymbol{\alpha}_{PT,k} \odot \mathbf{a}_{PT,k}$. The vector $\mathbf{a}_{PT,k} = [\exp(-j2\pi(R_{1T1,k}/\lambda), \exp(-j2\pi(R_{1T2,k}/\lambda), \cdots, \exp(-j2\pi(R_{mTn,k}/\lambda), \cdots, \exp(-j2\pi(R_{MTN,k}/\lambda)]^T$ is the

steering vector of PT_k. The operator $\odot$ is the Hadamard (element-wise) product. The first vector $\boldsymbol{\alpha}_{PT,k} = [\alpha_{11,k}, \alpha_{12,k}, \cdots, \alpha_{mn,k}, \cdots, \alpha_{MN,k}]^T$ is the amplitude vector of PT_k. The physical targets' echoes received by the widely distributed receivers are independent from each other due to the independence of RCS in different scattering directions. To simplify the subsequent derivation, as assumed in [18]–[20] and [22], $\alpha_{mn,k}$ is modelled as a complex Gaussian distributed random variable with zero mean and variance $\sigma^2_{PT,k}$. Therefore, $\boldsymbol{\alpha}_{PT,k} \sim \mathbb{CN}(\mathbf{0}_{MN\times 1}, \sigma^2_{PT,k}\mathbf{I}_{MN})$.

III. CORRELATION PROPERTY ANALYSIS

In this section, the mutual correlation property between false targets and the ones between physical and physical/false targets are analysed, which is the basis and prerequisite for the target discrimination.

In an inner product space, cosine similarity is a measure of similarity between two non-zero vectors that measures the cosine of the angle between them. In the complex vector space $\mathbb{C}^N$, the cosine of the complex-valued angle between two complex vectors $\mathbf{u}_1$ and $\mathbf{u}_2$ is defined as [27]

$$\cos(\theta_C) = \frac{\langle \mathbf{u}_1, \mathbf{u}_2 \rangle}{\|\mathbf{u}_1\| \, \|\mathbf{u}_2\|} \tag{9}$$

where $\langle \mathbf{u}_1, \mathbf{u}_2 \rangle = \mathbf{u}_1^H \mathbf{u}_2$ is the Hermitian product of $\mathbf{u}_1$ and $\mathbf{u}_2$. $\|\mathbf{u}_1\| = \sqrt{\langle \mathbf{u}_1, \mathbf{u}_1 \rangle}$ and $\|\mathbf{u}_2\| = \sqrt{\langle \mathbf{u}_2, \mathbf{u}_2 \rangle}$ are the norm of $\mathbf{u}_1$ and $\mathbf{u}_2$, respectively. H represents the complex conjugate transpose operation. (9) can be written as the following form [27]

$$\cos(\theta_C) = \rho \exp(-j\varphi) \tag{10}$$

where $\rho = \cos(\theta_H) = |\cos(\theta_C)|$. $0 \le \theta_H \le \pi/2$ and $-\pi \le \varphi \le \pi$ are the Hermitian and pseudo angle, respectively, between $\mathbf{u}_1$ and $\mathbf{u}_2$. The Hermitian angle between two complex vectors will do not change when multiplying the vectors by any complex scalars [28], which is an important property that can be used to discriminate physical and false targets. As analysed in the previous section, every false target signal vector can be expressed as the multiplication of a complex characterization factor and jamming steering vector. Therefore, the Hermitian angle between two arbitrary false target signal vectors will equal zero. Unfortunately, what we can obtain is the sample vectors with noise vectors rather than the false or physical target signal vectors, and the Hermitian angle between sample vectors is a complex statistical problem. To deal with this issue, the Hermitian distance between two complex vectors $\mathbf{u}_1$ and $\mathbf{u}_2$ is defined firstly, which is the cosine squared of the Hermitian angle between $\mathbf{u}_1$ and $\mathbf{u}_2$

$$HD(\mathbf{u}_1, \mathbf{u}_2) = \cos^2(\theta_H) = \left| \frac{\langle \mathbf{u}_1, \mathbf{u}_2 \rangle}{\|\mathbf{u}_1\| \, \|\mathbf{u}_2\|} \right|^2 \tag{11}$$

The reason choosing the cosine squared of the Hermitian angle rather than the cosine of Hermitian angle is that the statistical distribution properties of the former is easier to derive.

Then, the Hermitian distance is taken as the correlation metric to measure the mutual correlation property between false targets and the ones between physical and physical/false targets.

A. MUTUAL CORRELATION OF FALSE TARGETS VECTORS

Assume that there are two false targets, false target FT_1 and false target FT_2, and their sample vectors can be represented as

$$\mathbf{x}_{|FT,1} = \Gamma_1 \cdot \boldsymbol{\xi}_J + \mathbf{n}_1 \tag{12}$$

and

$$\mathbf{x}_{|FT,2} = \Gamma_2 \cdot \boldsymbol{\xi}_J + \mathbf{n}_2 \tag{13}$$

where the factors $\Gamma_1 = (\gamma_1 \lambda \sqrt{P_J})/(4\pi) \exp(-j2\pi f_0 \triangle \tau_1)$ and $\Gamma_2 = (\gamma_2 \lambda \sqrt{P_J})/(4\pi) \exp(-j2\pi f_0 \triangle \tau_2)$, which characterize the false target FT_1 and FT_2. The noise vectors $\mathbf{n}_1$ and $\mathbf{n}_2$ have the common distribution with $\mathbf{n}$, namely $\mathbf{n}_1 \sim \mathbb{CN}(\mathbf{0}_{MN\times 1}, \sigma_n^2 \mathbf{I}_{MN})$ and $\mathbf{n}_2 \sim \mathbb{CN}(\mathbf{0}_{MN\times 1}, \sigma_n^2 \mathbf{I}_{MN})$.

The correlation of FT_1 and FT_2 is the Hermitian distance between $\mathbf{x}_{|FT,1}$ and $\mathbf{x}_{|FT,2}$

$$HD(\mathbf{x}_{|FT,1}, \mathbf{x}_{|FT,2}) = \left| \frac{\langle \mathbf{x}_{|FT,1}, \mathbf{x}_{|FT,2} \rangle}{\|\mathbf{x}_{|FT,1}\| \, \|\mathbf{x}_{|FT,2}\|} \right|^2 \tag{14}$$

It is difficult to derive the exact probability distribution of $HD(\mathbf{x}_{|FT,1}, \mathbf{x}_{|FT,2})$. However, as is proved in Appendix A, the mean of $HD(\mathbf{x}_{|FT,1}, \mathbf{x}_{|FT,2})$ is expressed approximately as (15), as shown at the bottom of this page, where $\overline{JNR}_1 = \overline{En}_1/\sigma_n^2$ and $\overline{JNR}_2 = \overline{En}_2/\sigma_n^2$ are the average channel jamming-to-noise ratio (JNR) of FT_1 and FT_2, respectively.

$$\overline{En}_1 = \frac{|\Gamma_1|^2 \left|\boldsymbol{\xi}_J\right|^2}{MN} \tag{16}$$

and

$$\overline{En}_2 = \frac{|\Gamma_2|^2 \left|\boldsymbol{\xi}_J\right|^2}{MN} \tag{17}$$

are the average channel energy of FT_1 and FT_2, respectively. From (15), it is obvious that the the mean of $HD(\mathbf{x}_{|FT,1}, \mathbf{x}_{|FT,2})$ is only associated with the jammer power and has nothing to do with the modulation of false targets. The Hermitian distance between any two false targets increases with JNR.

$$E\left[HD(\mathbf{x}_{|FT,1}, \mathbf{x}_{|FT,2})\right] = \frac{\overline{JNR}_1 \cdot \overline{JNR}_2}{\left(\overline{JNR}_1 + 1\right) \cdot \left(\overline{JNR}_2 + 1\right)} + \frac{\overline{JNR}_1 + \overline{JNR}_2 + 1}{MN \cdot \left(\overline{JNR}_1 + 1\right) \cdot \left(\overline{JNR}_2 + 1\right)} \tag{15}$$

B. MUTUAL CORRELATION OF PHYSICAL AND PHYSICAL/FALSE TARGETS VECTORS

Assume that there are two physical targets, PT_1 and PT_2, whose sample vectors can be represented as

$$\mathbf{x}_{|PT,1} = \boldsymbol{\xi}_{PT,1} + \mathbf{n}_3 \tag{18}$$

and

$$\mathbf{x}_{|PT,2} = \boldsymbol{\xi}_{PT,2} + \mathbf{n}_4 \tag{19}$$

where the vectors $\boldsymbol{\xi}_{PT,1} \sim \mathbb{CN}(\mathbf{0}_{MN\times 1}, \sigma^2_{PT,1}\mathbf{I}_{MN})$ and $\boldsymbol{\xi}_{PT,2} \sim \mathbb{CN}(\mathbf{0}_{MN\times 1}, \sigma^2_{PT,2}\mathbf{I}_{MN})$ are the signal vector of PT_1 and PT_2, respectively. The noise vectors $\mathbf{n}_3$ and $\mathbf{n}_4$ have the common distribution with $\mathbf{n}$, namely $\mathbf{n}_3 \sim \mathbb{CN}(\mathbf{0}_{MN\times 1}, \sigma_n^2\mathbf{I}_{MN})$ and $\mathbf{n}_4 \sim \mathbb{CN}(\mathbf{0}_{MN\times 1}, \sigma_n^2\mathbf{I}_{MN})$.

The correlation of PT_1 and PT_2 is the Hermitian distance between $\mathbf{x}_{|PT,1}$ and $\mathbf{x}_{|PT,2}$

$$HD(\mathbf{x}_{|PT,1}, \mathbf{x}_{|PT,2}) = \left| \frac{\langle \mathbf{x}_{|PT,1}, \mathbf{x}_{|PT,2} \rangle}{\|\mathbf{x}_{|PT,1}\| \, \|\mathbf{x}_{|PT,2}\|} \right|^2 \tag{20}$$

Similarly, the correlation of PT_1 and FT_1 is

$$HD(\mathbf{x}_{|PT,1}, \mathbf{x}_{|FT,1}) = \left| \frac{\langle \mathbf{x}_{|PT,1}, \mathbf{x}_{|FT,1} \rangle}{\|\mathbf{x}_{|PT,1}\| \, \|\mathbf{x}_{|FT,1}\|} \right|^2 \tag{21}$$

As is proved in Appendix B that the Hermitian distance $HD(\mathbf{x}_{|PT,1}, \mathbf{x}_{|PT,2})$ and $HD(\mathbf{x}_{|PT,1}, \mathbf{x}_{|FT,1})$ have the same distribution, $HD(\mathbf{x}_{|PT,1}, \mathbf{x}_{|PT,2}) \sim Beta(1, MN-1)$ and $HD(\mathbf{x}_{|PT,1}, \mathbf{x}_{|FT,1}) \sim Beta(1, MN-1)$. $Beta(1, MN-1)$ is Beta distribution with shape parameters 1 and $MN-1$, whose probability density function (pdf) is

$$f(y) = (MN-1)(1-y)^{MN-2} \tag{22}$$

where $0 \le y \le 1$. It is obvious that the pdf $f(y)$ has nothing to do with signal or jamming power. Therefore, the mean of $HD(\mathbf{x}_{|PT,1}, \mathbf{x}_{|PT,2})$ and $HD(\mathbf{x}_{|PT,1}, \mathbf{x}_{|FT,1})$ is shown as Eq. (23), as shown at the bottom of this page, which is very different from the mean of $HD(\mathbf{x}_{|FT,1}, \mathbf{x}_{|FT,2})$. The variance of $HD(\mathbf{x}_{|PT,1}, \mathbf{x}_{|PT,2})$ and $HD(\mathbf{x}_{|PT,1}, \mathbf{x}_{|FT,1})$ is shown as (24), as shown at the bottom of this page, which is also constant.

IV. DISCRIMINATION METHOD

Based on the difference discussed in the previous section, we need to calculate the Hermitian distance between different vectors. In this section, we propose a new discrimination method by utilizing the difference of Hermitian distance, and deal with its theoretical discrimination performance.

A. PROPOSED DISCRIMINATOR

Assume that the total number of targets detected successfully in one monitoring is $K+Q$, their sample vectors being $\mathbf{x}_1$, $\mathbf{x}_2, \ldots, \mathbf{x}_{K+Q}$, in which the total numbers of physical targets and false targets are K and Q respectively. To identify the false targets, mutual correlation test between any two targets is needed to be performed based on the Hermitian distance. Therefore, the set of target combination can be represent as $\{(\mathbf{x}_i, \mathbf{x}_j) | i \ne j, \forall i, j = 1, 2, \ldots, K+Q\}$, and the set of Hermitian distance is written as $\{HD(\mathbf{x}_i, \mathbf{x}_j) | i \ne j, \forall i, j = 1, 2, \ldots, K+Q\}$. Considering $HD(\mathbf{x}_j, \mathbf{x}_i) = HD(\mathbf{x}_i, \mathbf{x}_j)$, $HD(\mathbf{x}_j, \mathbf{x}_i)$ can be obtained directly from $HD(\mathbf{x}_i, \mathbf{x}_j)$ without calculation. The target combination $(\mathbf{x}_i, \mathbf{x}_j)$ has three cases, which can be expressed as a multiple hypothesis testing (MHT) problem as following.

- The null hypothesis (H_0): the combination is composed of two false targets.
- The first hypothesis (H_1): the combination is composed of two physical targets.
- The second hypothesis (H_2): the combination is composed of a false target and a physical target.

Based on the difference of the Hermitian distances of different target combinations discussed in the previous section, the combination judgement is performed as

$$\begin{cases} \text{if } HD(\mathbf{x}_i, \mathbf{x}_j) \ge \mu : \text{accept } H_0 \\ \text{if } HD(\mathbf{x}_i, \mathbf{x}_j) < \mu : \text{accept } H_{12} \end{cases} \tag{25}$$

where μ is threshold, whose value will be dealt with in detail later, and H_{12} stands for the combination of H_1 and H_2. Each target will be tested with the number of $K+Q-1$.

Since the Hermitian distance has the same distribution under the hypotheses H_1 and H_2, the physical and false targets can not be discriminated under these cases. Therefore, the discrimination principle is that a target is accepted as a false target in the case that at least one of its $K+Q-1$ correlation tests is judged as H_0, otherwise, it is accepted as a physical target.

B. THEORETICAL PERFORMANCE ANALYSIS

To simplify the analysis, $\mathbb{S}_{PT}$ is defined as the physical target set consisting of all K sample vectors of physical targets. Similarly, $\mathbb{S}_{FT}$ is the false target set consisting of all Q sample vectors of false targets. The event A_k is defined as following

$$A_k : HD(\mathbf{x}_i, \mathbf{x}_k) < \mu \tag{26}$$

where $\mathbf{x}_i \in \mathbb{S}_{PT}$ and $\mathbf{x}_k$ is the kth vectors of the set $\{\mathbb{S}_{PT} \setminus \mathbf{x}_i\}$. $\setminus$ is the set subtraction operation. The event B_q is defined as

$$E\left[HD(\mathbf{x}_{|PT,1}, \mathbf{x}_{|PT,2})\right] = E\left[HD(\mathbf{x}_{|PT,1}, \mathbf{x}_{|FT,1})\right] = \frac{1}{MN} \tag{23}$$

$$D\left[HD(\mathbf{x}_{|PT,1}, \mathbf{x}_{|PT,2})\right] = D\left[HD(\mathbf{x}_{|PT,1}, \mathbf{x}_{|FT,1})\right] = \frac{MN-1}{(MN)^2(MN+1)} \tag{24}$$

following

$$B_q : HD(\mathbf{x}_i, \mathbf{x}_q) < \mu \tag{27}$$

where $\mathbf{x}_i \in \mathbb{S}_{PT}$ and $\mathbf{x}_q$ is the qth vectors of the set $\mathbb{S}_{FT}$.

According to the discrimination principle, the discrimination probability of a physical target, denoted by P_{PT}, is defined as the probability of accepting a physical target as a physical target, which can be written as

$$\begin{aligned} P_{PT} &\triangleq P\{\text{accepted as a PT}|\text{ a PT}\} \\ &= P\{\text{all correlation tests are judged as } H_{12}\} \\ &= P\{A_1A_2\cdots A_{K-1}B_1B_2\cdots B_Q\} \end{aligned} \tag{28}$$

Considering that the sample vectors of physical targets are mutually independent and independent from the ones of false targets, (28) can be rewritten as

$$\begin{aligned} P_{PT} &= P\{A_1A_2\cdots A_{K-1}\}\cdot P\{B_1B_2\cdots B_Q\} \\ &= P\{B_1B_2\cdots B_Q\}\cdot[P\{H_{12}|H_1\}]^{K-1} \end{aligned} \tag{29}$$

Although all false target signal vectors belong to a same vector space, $P_B = P\{B_1B_2\cdots B_Q\}$ is a complex issue with the effect of the random noise vectors. It is not easy to derive the exact expression of P_B, which is related to some unknown factors, such as JNR, the false target number. According to the JNR, the lower bound and the upper bound of P_B are given as $P_{B,lb}$ and $P_{B,ub}$, respectively.

$$\begin{cases} P_{B,lb} = P\{B_1\}P\{B_2\}\cdots P\{B_Q\}, \text{ with low JNR} \\ P_{B,ub} = P\{B_1\} = \cdots = P\{B_Q\}, \quad \text{with high JNR} \end{cases} \tag{30}$$

Therefore, the lower bound $P_{PT,lb}$ and the upper bound $P_{PT,ub}$ can be obtained as

$$\begin{aligned} P_{PT,lb} &= [P\{H_{12}|H_2\}]^Q\cdot[P\{H_{12}|H_1\}]^{K-1} \\ &= [\Phi_{Beta}(\mu)]^{K+Q-1} \end{aligned} \tag{31}$$

and

$$\begin{aligned} P_{PT,ub} &= P\{H_{12}|H_2\}\cdot[P\{H_{12}|H_1\}]^{K-1} \\ &= [\Phi_{Beta}(\mu)]^K \end{aligned} \tag{32}$$

respectively. $\Phi_{Beta}(\cdot)$ stands for the cumulative distribution function (CDF) of Beta distribution $Beta(1, MN-1)$ [29]

$$\Phi_{Beta}(\mu) = I_\mu(1, MN-1) \tag{33}$$

where $I_\mu(1, MN-1)$ is the regularized incomplete beta function.

The misjudgement probability of a physical target, denoted by P'_{PT}, is defined as

$$P'_{PT} \triangleq P\{\text{accepted as a FT}|\text{ a PT}\} = 1 - P_{PT} \tag{34}$$

Corresponding to $P_{PT,lb}$ and $P_{PT,ub}$, the upper bound $P'_{PT,ub}$ and the lower bound $P'_{PT,lb}$ are

$$\begin{aligned} P'_{PT,ub} &= 1 - P_{PT,lb} \\ &= 1 - [\Phi_{Beta}(\mu)]^{K+Q-1} \end{aligned} \tag{35}$$

and

$$\begin{aligned} P'_{PT,lb} &= 1 - P_{PT,ub} \\ &= 1 - [\Phi_{Beta}(\mu)]^K \end{aligned} \tag{36}$$

respectively. Because K and Q cannot be known in advance, $P_{PT,ub}$ is more suitable in the practice than $P_{PT,lb}$. With the cumulative distribution function Φ_{Beta} precisely known, $P_{PT,lb}$ and $P'_{PT,ub}$ can be obtained for a given μ, and vice versa. In other words, the discriminator proposed can restrict the upper bound of the misjudgement probability for physical targets. For a given expected misjudgement probability $P'_{PT,ub}$, μ can be calculated by

$$\mu = \Phi^{-1}_{Beta}\left(\left(1 - P'_{PT,ub}\right)^{1/(K+Q-1)}\right) \tag{37}$$

where $\Phi^{-1}_{Beta}(\cdot)$ is the inverse cumulative distribution function of the Beta distribution $Beta(1, MN-1)$.

Before discussing the discrimination probability of false targets, some definitions are given firstly. The event C_k is defined as following

$$C_k : HD(\mathbf{x}_i, \mathbf{x}_k) < \mu \tag{38}$$

where $\mathbf{x}_i \in \mathbb{S}_{FT}$ and $\mathbf{x}_k$ is the kth vectors of the set $\mathbb{S}_{PT}$. The event D_q is defined as

$$D_q : HD(\mathbf{x}_i, \mathbf{x}_q) < \mu \tag{39}$$

where $\mathbf{x}_i \in \mathbb{S}_{FT}$ and $\mathbf{x}_q$ is the qth vectors of the set $\{\mathbb{S}_{FT} \setminus \mathbf{x}_i\}$.

The discrimination probability of a false target, denoted by P_{FT}, is defined as the probability of accepting a false target as a false target, which can be written as

$$\begin{aligned} P_{FT} &\triangleq P\{\text{accepted as a FT}|\text{ a FT}\} \\ &= P\{\text{at least one of } K+Q-1 \text{ correlation} \\ &\qquad \text{tests is judged as } H_0\} \\ &= 1 - P\{C_1C_2\cdots C_KD_1D_2\cdots D_{Q-1}\} \\ &= 1 - P\{D_1D_2\cdots D_{Q-1}\}\cdot[P\{H_{12}|H_2\}]^K \\ &= 1 - P\{D_1D_2\cdots D_{Q-1}\}\cdot[\Phi_{Beta}(\mu)]^K \end{aligned} \tag{40}$$

where the probability $P\{D_1D_2\cdots D_{Q-1}\}$ is determined by the distribution of $HD(\mathbf{x}_i, \mathbf{x}_j)$ under H_0 and the JNR of false targets, similar to P_B. However, considering the distribution of $HD(\mathbf{x}_i, \mathbf{x}_j)$ under H_0 is unknown, the exact expression of P_{FT} is not given.

The discrimination method proposed is summarized as follows.

1) Threshold set: according to the (37), the threshold μ is set to restrict the upper bound of physical target misjudgement probability $P'_{PT,ub}$.
2) Correlation test: calculate the Hermitian distances of all the target combinations, and make judgement for every combination based on the (25).
3) Target discrimination: a target will be accepted as a false target in the case that at least one of its $K+Q-1$ correlation tests is judged as H_0, otherwise, it will be accepted as a physical target.

TABLE 1. Distributed multiple-radar architecture.

Transmitter/Receiver	Position / km
Z_T^1	$(5, 0, 0)$
Z_T^2	$(-5, 0, 0)$
Z_R^1	$(10, 0.5, 0)$
Z_R^2	$(-10, -0.2, 0)$
Z_R^3	$(0, 0, 0)$
Z_R^4	$(-4.5, 0.3, 0)$
Z_R^5	$(5, -0.3, 0)$

V. SIMULATION

In this section, a distributed multiple-radar architecture consisting of $M = 2$ transmitters and $N = 5$ receivers is considered. The positions of transmitters Z_T^m and receivers Z_R^n are set in kilometers as in Table 1. The carrier frequency is $f_0 = 1GHz$. The transmitting power of the transmitters is assumed as same. The antenna gains of all transmitters and receivers are also assumed as same.

There are a radar target, locating at $(1, 50, 10)$km, and a repeater jammer, locating at $(1.1, 51, 10)$km in the monitoring area. To protect the target, the jammer generates two false target around the target by implementing deception jamming. The jammer is also considered as a physical target. The focus of the section being on the analyses of the proposed discrimination method, so it is assumed that all the targets, including two physical targets and two false targets, have been successfully detected.

A. HERMITIAN DISTANCES OF DIFFERENT TARGET COMBINATIONS

In the subsection, the difference is verified firstly between Hermitian distances of different target combinations by Monte Carlo simulation.

As discussed in the Sec. III, the statistical characteristics of the Hermitian distance is related to the signal/jamming power. Therefore, some definitions are given firstly to make the presentation concise and easy to understand. The signal-to-noise ratio (SNR) of the physical target PT_k is defined as $SNR_k = \sigma_{PT,k}^2/\sigma_n^2$. The JNR of the false target FT_q is defined as the ratio of the jamming power to the noise power in the first transmit receive channel, denoted by $JNR_q = \left|\Gamma_q \cdot \boldsymbol{\xi}_J\{1\}\right|^2/\sigma_n^2$, where $\boldsymbol{\xi}_J\{1\}$ is the first element of the vector $\boldsymbol{\xi}_J$. The JNR in other channels can be obtained by the bi-static radar equation respectively. SNR_k $(k = 1, 2)$ and JNR_q $(q = 1, 2)$ are assumed as same, denoted by SNR.

In Fig. 1,the simulation results and theoretical values of the Hermitian distances under three hypotheses H_0, H_1 and H_2 are given versus different SNR. At each data point, the middle of the vertical bar is the simulation mean of the Hermitian distance, and the vertical bar stands for the standard deviation. Monte Carlo simulation is performed with 10^6 trials for each value of SNR.

It is obvious that the simulation mean of the Hermitian distance under the hypothesis H_0 gradually tends to its theoretical value with the rise of SNR, and its variance becomes smaller and smaller. The means of the Hermitian distances under the hypotheses H_1 and H_2 coincide with the the theoretical ones, and their means and variances are constant. Moreover, in Fig. 1b, the simulation results under H_1 and H_2 are consistent with the theory pdf, which validate the derivation in Sec. III. From the simulation results, the Hermitian distance under H_0 distinguishes clearly from the ones under H_1 and H_2. And the higher SNR is, the larger the difference is. Therefore, it is feasible to discriminate physical targets and false targets based on the difference.

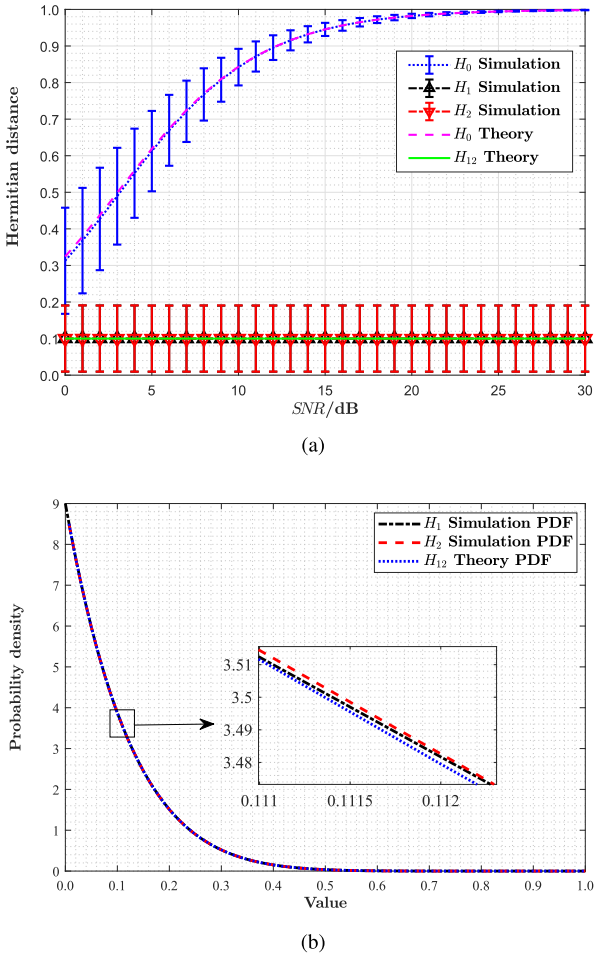

FIGURE 1. Hermitian distances under three hypotheses H_0, H_1 and H_2 (a) mean and standard deviation of Hermitian distances under three hypotheses (b) pdf of Hermitian distances under hypotheses H_1 and H_2.

B. PERFORMANCE OF THE PROPOSED DISCRIMINATION METHOD

The difference used to discriminate targets having been validated in the previous subsection, this subsection will prove the feasibility and superiority of the discrimination method proposed.

In the scenario assumed at the beginning of the section, the performance of the proposed method is firstly dealt with by simulations. In Fig. 2, the discrimination probabilities

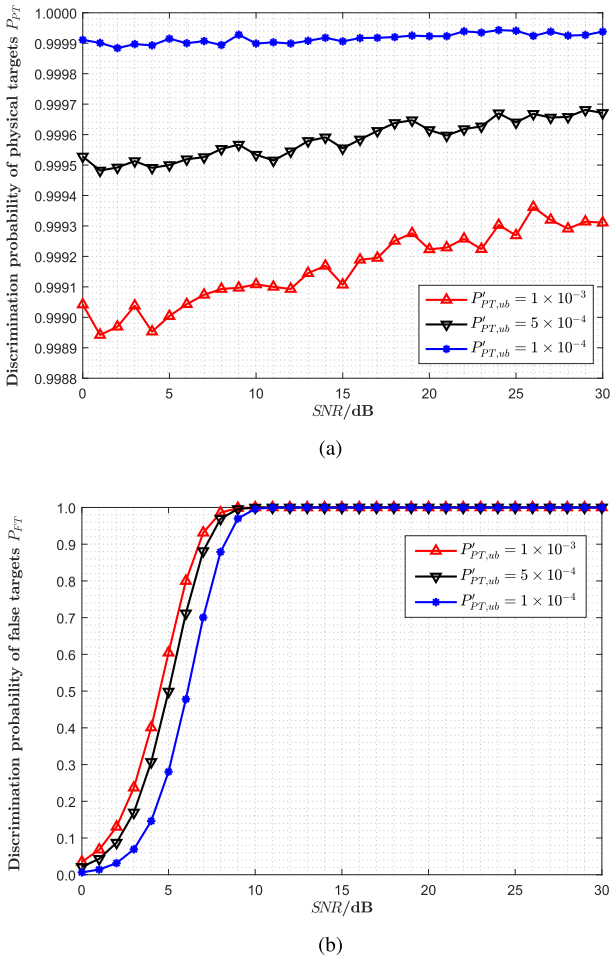

FIGURE 2. Discrimination performance of the proposed method (a) Discrimination probability of physical target P_{PT} (b) Discrimination probability of false target P_{FT}.

of targets P_{PT} and P_{FT} are given as a function of *SNR*. The curves correspond to different expected misjudgement probability $P'_{PT,ub}$, where $P'_{PT,ub} = 1\times10^{-3}, 5\times10^{-4}$ and 1×10^{-4}. All performance curves are obtained by averaging over 10^6 independent Monte Carlo runs at each value of *SNR*.

From the simulation result, the proposed method can discriminate the physical targets and false targets effectively. Under the condition $P'_{PT,ub} = 1\times10^{-3}$, the threshold is calculated as $\mu \approx 0.5892$ based on (37). Therefore, the theoretical lower bound and upper bound of the discrimination probability of physical target are $P_{PT,lb} = 1 - P'_{PT,ub} = 0.999$ and $P_{PT,ub} \approx 0.9993$, respectively. For $P'_{PT,ub} = 1\times10^{-3}$, as shown in Fig. 2a, the discrimination probability of physical target P_{PT} fluctuates around the theoretical lower bound $P_{PT,lb}$ at low *SNR*. With the increasing of *SNR*, P_{PT} gradually approaches and fluctuates around the theoretical upper bound $P_{PT,ub}$. The simulation misjudgement probability of physical targets is approximately in the range $[1 - P_{PT,ub}, P'_{PT,ub}]$. And so are the cases with other values of $P'_{PT,ub}$. Coinciding with the theoretical analysis in Sec. IV, the proposed method can restrict the upper bound of the misjudgement probability for physical targets. The difference between the lower bound and the upper bound of probability P_{PT} decreases with the decreasing of probability $P'_{PT,ub}$. With a lower $P'_{PT,ub}$, the proposed method can obtain an approximate constant misjudgement probability for physical targets. In Fig. 2b, for a same $P'_{PT,ub}$, the higher *SNR* is, the greater the discrimination probability of false targets P_{FT} is. This is because the difference between physical targets and false targets becomes larger with *SNR*. At low *SNR*, the higher $P'_{PT,ub}$, the smaller the threshold μ, the greater the probability P_{FT}. From the simulation results, for $P'_{PT,ub} = 1\times10^{-3}$, the probability P_{FT} has been much bigger than 0.95 when *SNR* = 8dB and almost reaches to 1 when *SNR* = 10dB. It is needed a little higher *SNR* for other values of $P'_{PT,ub}$ to obtain the same probability P_{FT}. For a smaller probability $P'_{PT,ub}$, the proposed method still obtains accepted discriminate probability for false targets, especially for the case with *SNR* larger than 12dB.

As a contrast, the simulation results of the method in [22] are given in the same scenario. As mentioned in Sec. I, the location precision for the jammer has a significant effect on the performance of the method in [22]. In the Cartesian coordinate system, the three-dimensional location errors for the jammer are assumed to be independent identical Gaussian distribution $N(0, \sigma_e^2)$. In Fig. 3, the discrimination probabilities of targets P_{PT} and P_{FT} are given as a function of *SNR* with different location errors. The misjudgement probability of false target is set 1×10^{-3}. The curves correspond to different location error σ_e, where $\sigma_e = 0, 0.5\lambda, \lambda, 10\lambda$. In this simulation, $\lambda = 0.3$m.

As shown in Fig. 3a, the location error has no effect on the discrimination probabilities of physical target P_{PT}. Although the location error for the jammer leads to the estimation error of the jamming feature matrix $\mathbf{A}$, the characteristics of the physical target signal vector $\boldsymbol{\xi}_{PT,k}$ determines that the relationship $\mathbf{A}\boldsymbol{\xi}_{PT,k} \neq \mathbf{0}$ never changes with $\mathbf{A}$. Therefore, P_{PT} won't be impacted at all. However, comparing Fig. 3a and 2a, the performance of the proposed method possesses better performance than the available method. And in Fig. 3b, when there are location errors, the discrimination performance for false targets deteriorates drastically with the increase of location errors and *SNR*. Location errors make the relationship $\mathbf{A}\boldsymbol{\xi}_{FT,q} = \mathbf{0}$ not hold, which will lead to the energy residue of false targets after projection. The greater the location errors and *SNR*, the more the energy residue, and the greater the probability of judging false targets as physical targets. It's almost intolerable that P_{FT} is below 0.5 when *SNR* $\geq$ 2dB and $\sigma_e = 10\lambda$.

Compared with the method in [22], firstly, the proposed method does not require any prior information about the jammer, which makes the proposed method more practical. Secondly, the proposed method can restrict the upper bound of the misjudgement probability for physical targets, which is extremely important for that the cost of misjudging physical targets is much higher than that of misjudging false targets.

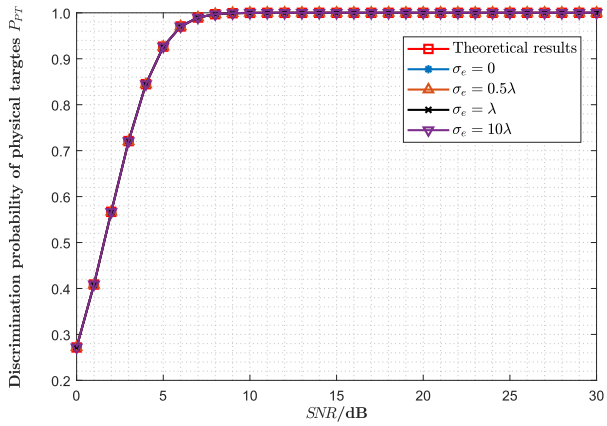

(a)

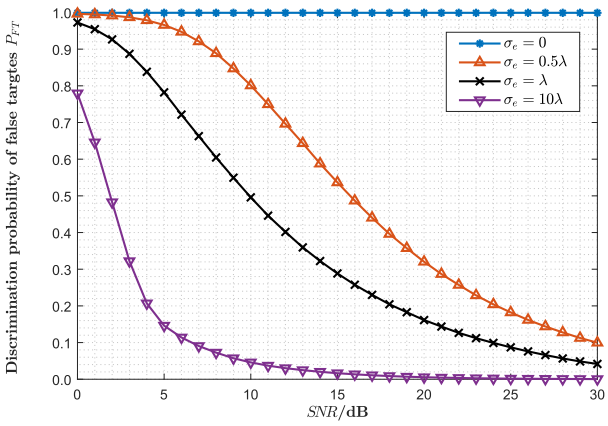

(b)

FIGURE 3. Discrimination performance of the method in [22] (a) Discrimination probability of physical target P_{PT} (b) Discrimination probability of false target P_{FT}.

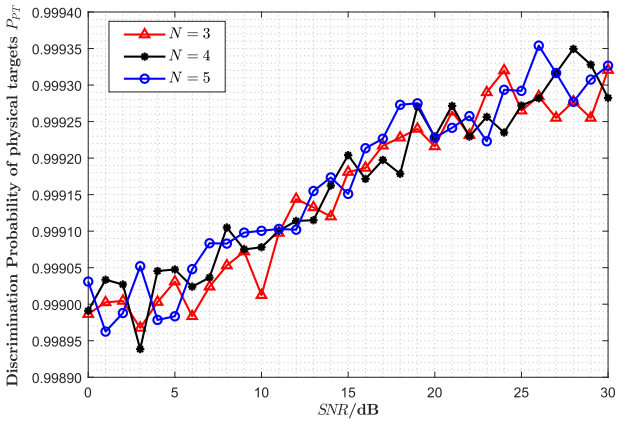

(a)

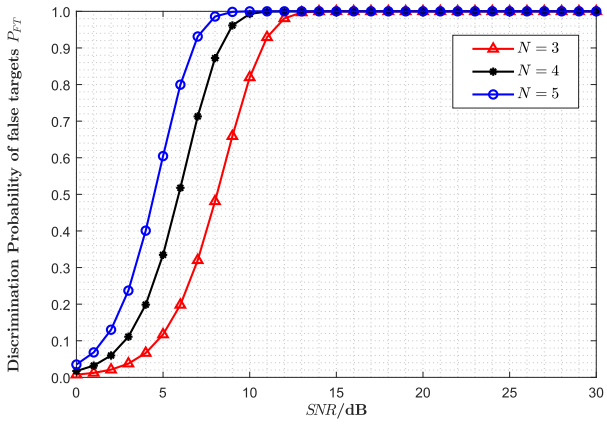

(b)

FIGURE 4. Discrimination performance of the proposed method with different numbers of receivers (a) Discrimination probability of physical target P_{PT} (b) Discrimination probability of false target P_{FT}.

C. INFLUENCE OF CHANNEL NUMBER AND FALSE TARGET NUMBER

As discussed in Sec. III and Sec. IV, the Hermitian distances of different target combinations are affected by the channel number and the theoretical performance of the proposed method is related to the false target number. Therefore, this subsection deals with their influence on the performance by simulation.

In Fig. 4, the discrimination probabilities of targets P_{PT} and P_{FT} are given as a function of *SNR* with different numbers of receivers. The expected misjudgement probability of physical target is set $P'_{PT,ub} = 1\times10^{-3}$. The curves correspond to different numbers of receivers N, where $N = 3, 4, 5$. When $N = 3$, the first three receivers (i.e. Z_R^1, Z_R^2, and Z_R^3) are used, and when $N = 4$, the first four receivers are used except Z_R^5.

As shown in Fig. 4a, the channel number has little impact on the discrimination probabilities of physical targets. Actually, according to (31) and (32), the probability P_{PT} is determined by the function $\Phi_{Beta}(\mu)$ for given K and Q. However, for different channel numbers, the function $I_\mu(1, MN)$ has little difference when the probability $P'_{PT,ub} = 1 \times 10^{-3}$. From Fig. 4b, it is obvious that the larger the channel number, the greater the discrimination probability of false targets P_{FT}. According to (15) and (23), although both Hermitian distances under H_0 and H_{12} decrease with the increase of channel number, the Hermitian distance under H_{12} reduces more than that under H_0. Besides, the Hermitian distance under H_0 has lower bound due to the first term on the right hand side of (15). In other words, the difference between the Hermitian distances of different target combination becomes greater in a higher-dimensional space.

In Fig. 5, the discrimination probabilities of targets P_{PT} and P_{FT} are given as a function of *SNR* with different numbers of false targets. The expected misjudgement probability of physical target is also set $P'_{PT,ub} = 1 \times 10^{-3}$. The curves correspond to different numbers of false targets Q, where $Q = 2, 5, 8$.

It is apparent in Fig. 5a that the upper bound of the discrimination probability for physical targets $P_{PT,ub}$ increases with false targets number Q. The lower bound $P_{PT,lb} = 1-P'_{PT,ub}$ is same for all cases with different Q for a given expected misjudgement probability $P'_{PT,ub}$. According to (37) and (32),

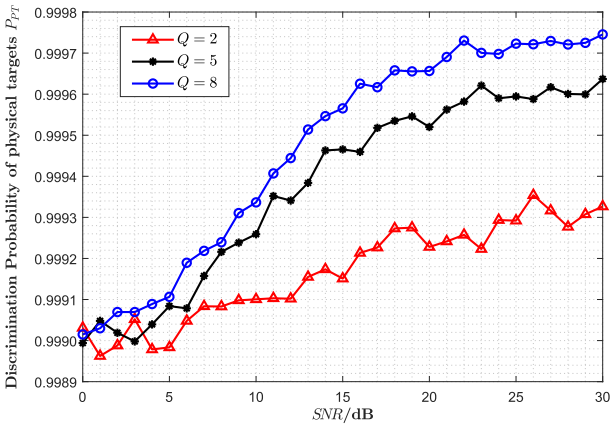

(a)

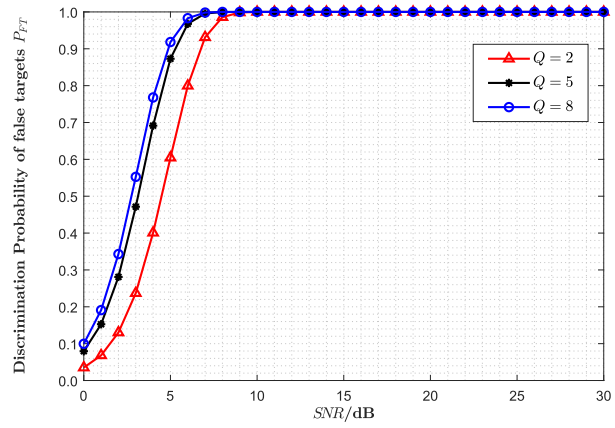

(b)

FIGURE 5. Discrimination performance of the proposed method with different numbers of false targets (a) Discrimination probability of physical target P_{PT} (b) Discrimination probability of false target P_{FT}.

the more the false targets, the greater the threshold, thus the greater the upper probability $P_{PT,ub}$. In Fig. 5b, a better discrimination performance for false targets is obtained with more false targets. The more the false targets, the more mutual correlation tests performed, the greater discrimination probability for false targets.

VI. CONCLUSION

The difference of targets' spatial scattering property has a new manifestation in the distributed multiple-radar architecture, which is that the Hermitian distance between any two false targets generated by a same jammer is larger than that between any other target combinations. Based on the difference, a discrimination method is proposed to discriminate physical targets and false targets. The theoretical analysis and simulation verify the feasibility and validity of the discrimination method proposed. Compared with the available methods, the proposed method does not require any prior information about the jamming environment and can discriminate the targets effectively in one PRI. Moreover, the proposed method can restrict the upper bound of the misjudgement probability for physical targets.

However, the proposed discrimination method is based on the difference in Hermitian distances of different target combinations, and the Hermitian distance between two physical targets and the one between a physical target and a false target have a same distribution as analyzed in Sec. III, which means that the false target cannot be discriminated in the case with only one false target. Therefore, the proposed method is applicable to the case with two or multiple false targets. How to discriminate the false target in one false target case will be the subsequent work.

APPENDIX A
DERIVATION OF (15)

The mean of the correlation between FT_1 and FT_2 is

$$\begin{aligned}
&E\left[HD(\mathbf{x}_{|FT,1}, \mathbf{x}_{|FT,2})\right] \\
&= E\left[\left|\frac{\left\langle \mathbf{x}_{|FT,1}, \mathbf{x}_{|FT,2}\right\rangle}{\left\|\mathbf{x}_{|FT,1}\right\| \left\|\mathbf{x}_{|FT,2}\right\|}\right|^2\right] \\
&= E\left[\frac{\left(\mathbf{x}_{|FT,1}^H \mathbf{x}_{|FT,2}\right)^H \left(\mathbf{x}_{|FT,1}^H \mathbf{x}_{|FT,2}\right)}{\left(\mathbf{x}_{|FT,1}^H \mathbf{x}_{|FT,1}\right)\left(\mathbf{x}_{|FT,2}^H \mathbf{x}_{|FT,2}\right)}\right] \\
&= \frac{|\Gamma_1|^2 |\Gamma_2|^2 \left|\boldsymbol{\xi}_J\right|^4 + \sigma_n^2 |\Gamma_1|^2 \left|\boldsymbol{\xi}_J\right|^2}{\left(|\Gamma_1|^2 \left|\boldsymbol{\xi}_J\right|^2 + MN\sigma_n^2\right)\left(|\Gamma_2|^2 \left|\boldsymbol{\xi}_J\right|^2 + MN\sigma_n^2\right)} \\
&\quad + \frac{\sigma_n^2 |\Gamma_2|^2 \left|\boldsymbol{\xi}_J\right|^2 + MN\sigma_n^4}{\left(|\Gamma_1|^2 \left|\boldsymbol{\xi}_J\right|^2 + MN\sigma_n^2\right)\left(|\Gamma_2|^2 \left|\boldsymbol{\xi}_J\right|^2 + MN\sigma_n^2\right)}
\end{aligned} \tag{41}$$

Noticing that $|\Gamma_1|^2 \left|\boldsymbol{\xi}_J\right|^2$ is FT_1's total energy of all MN transmitter-receiver channels, which can be simplified as $|\Gamma_1|^2 \left|\boldsymbol{\xi}_J\right|^2 = MN \cdot \overline{En_1}$. $\overline{En_1}$ is the average channel energy of FT_1. Similarly, $|\Gamma_2|^2 \left|\boldsymbol{\xi}_J\right|^2 = MN \cdot \overline{En_2}$ is FT_2's total energy and $\overline{En_2}$ is its average channel energy. Therefore, (41) can be rewritten as

$$\begin{aligned}
&E\left[HD(\mathbf{x}_{|FT,1}, \mathbf{x}_{|FT,2})\right] \\
&\quad = \frac{MN \cdot \overline{JNR_1} \cdot \overline{JNR_2} + \overline{JNR_1} + \overline{JNR_2} + 1}{MN \cdot \left(\overline{JNR_1} + 1\right) \cdot \left(\overline{JNR_2} + 1\right)}
\end{aligned} \tag{42}$$

where $\overline{JNR_1} = \overline{En_1}/\sigma_n^2$ and $\overline{JNR_2} = \overline{En_2}/\sigma_n^2$ are the average channel jamming-to-noise ratio (JNR) of the false target FT_1 and FT_2, respectively.

APPENDIX B
THE DISTRIBUTION OF HERMITIAN DISTANCE UNDER H_1 AND H_2

Since the vectors $\boldsymbol{\xi}_{PT,1}$, $\boldsymbol{\xi}_{PT,2}$, $\mathbf{n}_3$ and $\mathbf{n}_4$ are independent complex Gaussian vectors, $\mathbf{x}_{|PT,1} \sim \mathbb{CN}(\mathbf{0}_{MN\times 1}, (\sigma_{PT,1}^2 + \sigma_n^2)\mathbf{I}_{MN})$ and $\mathbf{x}_{|PT,2} \sim \mathbb{CN}(\mathbf{0}_{MN\times 1}, (\sigma_{PT,2}^2 + \sigma_n^2)\mathbf{I}_{MN})$. The normalized vectors $\mathbf{S}_{MN} = \mathbf{x}_{|PT,1}/\|\mathbf{x}_{|PT,1}\|$, $\mathbf{S}_{MN}^1 = \mathbf{x}_{|PT,2}/\|\mathbf{x}_{|PT,2}\|$ and $\mathbf{S}_{MN}^2 = \mathbf{x}_{|FT,1}/\|\mathbf{x}_{|FT,1}\|$ locate on the

$MN-1$ dimensional unit complex sphere S^{MN-1}. It is satisfied that

$$HD(\mathbf{x}_{|PT,1}, \mathbf{x}_{|PT,2}) = HD(\mathbf{S}_{MN}, \mathbf{S}^1_{MN}) = \left|\left\langle \mathbf{S}_{MN}, \mathbf{S}^1_{MN} \right\rangle\right|^2 \quad (43)$$

and

$$HD(\mathbf{x}_{|PT,1}, \mathbf{x}_{|FT,1}) = HD(\mathbf{S}_{MN}, \mathbf{S}^2_{MN}) = \left|\left\langle \mathbf{S}_{MN}, \mathbf{S}^2_{MN} \right\rangle\right|^2 \quad (44)$$

If $\mathbf{Y} \sim \mathbb{CN}(\mathbf{0}_{n\times 1}, \mathbf{I}_n)$, then $\mathbf{S}_n = \mathbf{Y}/\|\mathbf{Y}\|$ will uniformly distribute on the $n-1$ dimensional unit complex sphere S^{n-1}, which is an extension to complex value case of [30]. Therefore, $\mathbf{S}_{MN}$ uniformly distribute on the unit complex sphere S^{MN-1}. For an arbitrary point $\mathbf{S}'_{MN}$ on the unit complex sphere S^{MN-1}, $\langle \mathbf{S}_{MN}, \mathbf{S}'_{MN} \rangle = \langle \mathbf{F}_1 \cdot \mathbf{S}_{MN}, \mathbf{F}_1 \cdot \mathbf{S}'_{MN} \rangle = \langle \mathbf{F}_1 \cdot \mathbf{S}_{MN}, \mathbf{e}_1 \rangle$ is satisfied for the rotational invariance property. $\mathbf{e}_1 = [1, 0, 0, \ldots, 0]^T$ is the first coordinate unit vector, and $\mathbf{F}_1$ is the transformation matrix to rotate $\mathbf{S}'_{MN}$ to $\mathbf{e}_1$. $\mathbf{S}_{MN}$ distributing uniformly on the unit complex sphere S^{MN-1}, it will still distribute uniformly after any rotation, namely $\mathbf{F}_1 \cdot \mathbf{S}_{MN}$ distributes uniformly on the unit complex sphere S^{MN-1}. Therefore, $\langle \mathbf{F}_1 \cdot \mathbf{S}_{MN}, \mathbf{e}_1 \rangle$ has the same distribution with $\langle \mathbf{S}_{MN}, \mathbf{e}_1 \rangle$. Meanwhile, it is obvious that the distribution of $\mathbf{S}'_{MN}$ has no effect on the distribution of $\left\langle \mathbf{S}_{MN}, \mathbf{S}'_{MN} \right\rangle$. Hence, $HD(\mathbf{x}_{|PT,1}, \mathbf{x}_{|PT,2})$ and $HD(\mathbf{x}_{|PT,1}, \mathbf{x}_{|FT,1})$ have the same distribution with $HD(\mathbf{S}_{MN}, \mathbf{e}_1)$.

$HD(\mathbf{S}_{MN}, \mathbf{e}_1)$ is the Hermitian distance between $\mathbf{S}_{MN}$ and $\mathbf{e}_1$

$$HD(\mathbf{S}_{MN}, \mathbf{e}_1) = |\langle \mathbf{S}_{MN}, \mathbf{e}_1 \rangle|^2 = |h_1|^2 \quad (45)$$

where h_1 is the first element of $\mathbf{S}_{MN}$. The probability

$$P\left(HD(\mathbf{S}_{MN}, \mathbf{e}_1) \le y\right) = P\left(|h_1|^2 \le y\right) = \frac{A_h}{A_S} \quad (46)$$

where A_S is surface area of the $MN-1$ dimensional unit complex sphere S^{MN-1} [31] is

$$A_S = \frac{2\pi^{MN}}{2^{MN}(MN-1)!} \quad (47)$$

and A_h is the area of the spherical cap formed by the intersection of the subspace $|h_1| < \sqrt{y}$ [31] is

$$A_h = \frac{2\pi^{MN}}{2^{MN}(MN-1)!}\left(1-(1-y)^{MN-1}\right) \quad (48)$$

Therefore,

$$P\left(HD(\mathbf{S}_{MN}, \mathbf{e}_1) \le y\right) = 1-(1-y)^{MN-1} \quad (49)$$

Then, the pdf of $HD(\mathbf{S}_{MN}, \mathbf{e}_1)$ is obtained by differentiating $P\left(HD(\mathbf{S}_{MN}, \mathbf{e}_1) \le y\right)$ given by

$$f(y) = (MN-1)(1-y)^{MN-2} \quad (50)$$

which happens to be Beta distribution $Beta(1, MN-1)$.

Therefore, $HD(\mathbf{x}_{|PT,1}, \mathbf{x}_{|PT,2})$ and $HD(\mathbf{x}_{|PT,1}, \mathbf{x}_{|FT,1})$ obey a same Beta distribution, $HD(\mathbf{x}_{|PT,1}, \mathbf{x}_{|PT,2}) \sim Beta(1, MN-1)$ and $HD(\mathbf{x}_{|PT,1}, \mathbf{x}_{|FT,1}) \sim Beta(1, MN-1)$.

REFERENCES

[1] S. J. Roome, "Digital radio frequency memory," *Electron. Commun. Eng. J.*, vol. 2, no. 4, pp. 147–153, Aug. 1990.
[2] S. D. Berger, "Digital radio frequency memory linear range gate stealer spectrum," *IEEE Trans. Aerosp. Electron. Syst.*, vol. 39, no. 2, pp. 725–735, Apr. 2003.
[3] A. Farina, "Electronic counter-countermeasures," in *Radar Handbook*, 3rd ed. M. I. Skolnik, Ed. New York, NY, USA: McGraw-Hill, 2008.
[4] M. Greco, F. Gini, and A. Farina, "Radar detection and classification of jamming signals belonging to a cone class," *IEEE Trans. Signal Process.*, vol. 56, no. 5, pp. 1984–1993, May 2008.
[5] F. Bandiera, A. Farina, D. Orlando, and G. Ricci, "Detection algorithms to discriminate between radar targets and ecm signals," *IEEE Trans. Signal Process.*, vol. 58, no. 12, pp. 5984–5993, Dec. 2010.
[6] J. Akhtar, "Orthogonal block coded ECCM schemes against repeat radar jammers," *IEEE Trans. Aerosp. Electron. Syst.*, vol. 45, no. 3, pp. 1218–1226, Jul. 2009.
[7] B. Rao, Y.-L. Zhao, S.-P. Xiao, and X.-S. Wang, "Discrimination of exo-atmospheric active decoys using acceleration information," *IET Radar, Sonar Navigat.*, vol. 4, no. 4, pp. 626–638, 2010.
[8] B. Rao, S. Xiao, and X. Wang, "Joint tracking and discrimination of exoatmospheric active decoys using nine-dimensional parameter-augmented EKF," *Signal Process.*, vol. 91, no. 10, pp. 2247–2258, Oct. 2011.
[9] B. Rao, S. Xiao, X. Wang, and T. Wang, "Maximum likelihood approach to the estimation and discrimination of exoatmospheric active phantom tracks using motion features," *IEEE Trans. Aerosp. Electron. Syst.*, vol. 48, no. 1, pp. 794–819, Jan. 2012.
[10] G. Cui, X. Yu, Y. Yuan, and L. Kong, "Range jamming suppression with a coupled sequential estimation algorithm," *IET Radar, Sonar Navigat.*, vol. 12, no. 3, pp. 341–347, Mar. 2018.
[11] P. Stavroulakis, N. Farsaris, and T. D. Xenos, "Anti-jamming transmitter independent radar networks," in *Proc. Int. Conf. Signal Process., Commun. Netw.*, Jan. 2008, pp. 269–273.
[12] S. Z. Yanglin, "Identification of false targets in bistatic radar system," in *Proc. IEEE NAECON*, Dayton, OH, USA, vol. 2, Jul. 1997, pp. 878–883.
[13] Y. Zhao, X. Wang, G. Wang, Y. Liu, and J. Luo, "Tracking technique for radar network in the presence of multi-range-false-target deception jamming," *Acta Electron. Sinica*, vol. 35, no. 3, pp. 454–458, 2007.
[14] B. Lv, Y. Song, and C.-Y. Zhou, "Study of multistatic radar against velocity-deception jamming," in *Proc. ICECC*, Ningbo, China, Sep. 2011, pp. 1044–1047.
[15] D. Huang, G. Cui, X. Yu, M. Ge, and L. Kong, "Joint range–velocity deception jamming suppression for SIMO radar," *IET Radar, Sonar Navigat.*, vol. 13, no. 1, pp. 113–122, 2019.
[16] E. Fishler, A. Haimovich, R. S. Blum, L. J. Cimini, D. Chizhik, and R. A. Valenzuela, "Spatial diversity in radars-models and detection performance," *IEEE Trans. Signal Process.*, vol. 54, no. 3, pp. 823–838, Mar. 2006.
[17] S. Zhou, H. Liu, Y. Zhao, and L. Hu, "Target spatial and frequency scattering diversity property for diversity MIMO radar," *Signal Process.*, vol. 91, no. 2, pp. 269–276, 2011.
[18] S. Zhao, L. Zhang, Y. Zhou, N. Liu, and J. Liu, "Discrimination of active false targets in multistatic radar using spatial scattering properties," *IET Radar, Sonar Navigat.*, vol. 10, no. 5, pp. 817–826, 2016.
[19] S. Zhao, L. Zhang, Y. Zhou, and N. Liu, "Signal fusion-based algorithms to discriminate between radar targets and deception jamming in distributed multiple-radar architectures," *IEEE Sensors J.*, vol. 15, no. 11, pp. 6697–6706, Nov. 2015.
[20] S. Zhao, N. Liu, L. Zhang, Y. Zhou, and Q. Li, "Discrimination of deception targets in multistatic radar based on clustering analysis," *IEEE Sensors J.*, vol. 16, no. 8, pp. 2500–2508, Apr. 2016.
[21] B. Wang, G. Cui, S. Zhang, B. Sheng, L. Kong, and D. Ran, "Deceptive jamming suppression based on coherent cancelling in multistatic radar system," in *Proc. IEEE Radar Conf. (RadarConf)*, May 2016, pp. 1–5.
[22] S. Zhao, Y. Zhou, L. Zhang, Y. Guo, and S. Tang, "Discrimination between radar targets and deception jamming in distributed multiple-radar architectures," *IET Radar, Sonar Navigat.*, vol. 11, no. 7, pp. 1124–1131, 2017.
[23] H. Deng, "Polyphase code design for Orthogonal Netted Radar systems," *IEEE Trans. Signal Process.*, vol. 52, no. 11, pp. 3126–3135, Nov. 2004.
[24] W. Li, H. Leung, and Y. Zhou, "Space-time registration of radar and ESM using unscented Kalman filter," *IEEE Trans. Aerosp. Electron. Syst.*, vol. 40, no. 3, pp. 824–836, Jul. 2004.

[25] D. R. Brown, III, and H. V. Poor, "Time-slotted round-trip carrier synchronization for distributed beamforming," *IEEE Trans. Signal Process.*, vol. 56, no. 11, pp. 5630–5643, Nov. 2008.
[26] W. Wang, "GPS-based time & Phase synchronization processing for distributed SAR," *IEEE Trans. Aerosp. Electron. Syst.*, vol. 45, no. 3, pp. 1040–1051, Jul. 2009.
[27] K. Scharnhorst, "Angles in complex vector spaces," *Acta Applicandae Math.*, vol. 69, no. 1, pp. 95–103, Oct. 2001.
[28] V. G. Reju, S. N. Koh, and I. Y. Soon, "Underdetermined convolutive blind source separation via time–frequency masking," *IEEE Trans. Audio, Speech, Language Process.*, vol. 18, no. 1, pp. 101–116, Jan. 2010.
[29] C. Walck, "Beat distribution," in *Handbook Statistical Distribution for Experimentalists*. Stockholm, Sweden: Univ. Stockholm, Sep. 2008.
[30] M. E. Müller, "A note on a method for generating points uniformly on N-dimensional spheres," *Commun. Assoc. Comput. Mach.*, vol. 2, pp. 19–20, Apr. 1959.
[31] K. K. Mukkavilli, A. Sabharwal, E. Erkip, and B. Aazhang, "On beamforming with finite rate feedback in multiple-antenna systems," *IEEE Trans. Inf. Theory*, vol. 49, no. 10, pp. 2562–2579, Oct. 2003.

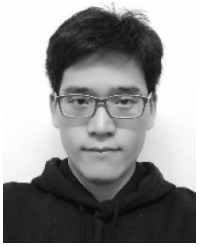

QIANG LI was born in Shandong, China. He is currently pursuing the Ph.D. degree in signal processing with the National Laboratory of Radar Signal Processing, Xidian University, Xi'an, China.

His research interests include statistical signal processing, array signal processing, and electronic counter-countermeasure in multiple radar systems.

LINRANG ZHANG was born in Shaanxi, China, in 1966. He received the M.S. and Ph.D. degrees in electrical engineering from Xidian University, China, in 1991 and 1999, respectively.

He is currently a Full Professor with the National Laboratory of Radar Signal Processing, Xidian University. He has authored or coauthored three books and published over 100 papers. His research interests include radar system analysis and simulation, radar signal processing, and jamming suppression.

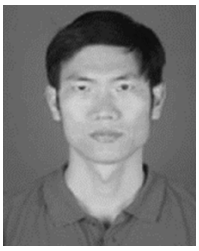

YU ZHOU received the M.S. and Ph.D. degrees from Xidian University, Xi'an, China, in 2004 and 2011, respectively.

He is currently an Associate Professor with the National Laboratory of Radar Signal Processing, Xidian University. His current research interests include ground moving target indication, spectrum sharing cognitive radar signal processing, and multiple input multiple output radar.

SHANSHAN ZHAO received the Ph.D. degree from the National Laboratory of Radar Signal Processing, Xidian University, in 2016.

She is currently a Lecturer with the College of Electronic and Optical Engineering, Nanjing University of Posts and Telecommunications, Nanjing, China. Her research interests include statistical signal processing, information fusion in multisite radar systems, and their application in radar ECCM.

NAN LIU received the B.S. and Ph.D. degrees from Xidian University, Xi'an, China, in 2004 and 2009, respectively.

He is currently an Associate Professor with the National Laboratory of Radar Signal Processing, Xidian University. His current research interests include array signal processing, multiple input multiple output radar, and radar electronic counter-countermeasure.

JUAN ZHANG received the B.S., M.S., and Ph.D. degrees from Xidian University, Xi'an, China, in 2003, 2006, and 2010, respectively.

She is currently an Associate Professor with the National Laboratory of Radar Signal Processing, Xidian University. Her current research interests include array signal processing, multiple input multiple output radar, radar electronic counter-countermeasure, and multipath signal processing.